

Assessment of Common Simulation Protocols for Simulations of Nanopores, Membrane Proteins, and Channels

Jirasak Wong-ekkabut^{*,†} and Mikko Karttunen^{*,‡}

[†]Department of Physics, Faculty of Science, Kasetsart University, 50 Phahon Yothin Road, Chatuchak, Bangkok 10900, Thailand

[‡]Department of Chemistry, University of Waterloo, 200 University Avenue West, Waterloo, Ontario, Canada N2L 3G1

ABSTRACT: Molecular dynamics (MD) simulation has become a common technique to study biological systems. Transport of small molecules through carbon nanotubes and membrane proteins has been an intensely studied topic, and MD simulations have been able to provide valuable predictions, many of which have later been experimentally proven. Simulations of such systems pose challenges, and unexpected problems in commonly used protocols and methods have been found in the past few years. The two main reasons why some were not found before are that most of these newly discovered errors do not lead to unstable simulations. Furthermore, some of them manifest themselves only after relatively long simulation times. We assessed the reliability of the most common simulations protocols by MD and stochastic dynamics (SD) or Langevin dynamics, simulations of an alpha hemolysin nanochannel embedded in a palmitoylcholine (POPC) lipid bilayer. Our findings are that (a) reaction field electrostatics should not be used in simulations of such systems, (b) local thermostats should be preferred over global ones since the latter may lead to an unphysical temperature distribution, (c) neighbor lists should be updated at all time steps, and (d) charge groups should be used with care and never in conjunction with reaction field electrostatics.

INTRODUCTION

Molecular dynamics (MD) simulation is a powerful technique to study the structures, dynamics, and interactions of biological molecules.^{1–3} It has been successful in predicting physical phenomena such as the ability of water molecules to penetrate carbon nanotubes^{4,5} and the collective nature of lipid diffusion.⁶ Simulations can be quantitative and predictive: Both of the above predictions and many others have been later verified by experiments.⁷ Simulations can also tell how probes used in experiments may disturb^{8,9} the system and hence help to provide a more accurate interpretation of experiments.

Like all techniques, MD simulation has both advantages and disadvantages. Algorithmic properties are one concern,¹⁰ but over the past years force fields^{11–21} and methodological issues such as how to include long-range electrostatic interactions^{22–37} accurately and reliably and the long-time stability of simulations have been the main concerns. Efforts for more quantitative and accurate modeling have led to improved scrutiny of the methods, and the past couple of years have provided surprises: Bonthuis et al.^{38,39} found that truncation of the Lennard–Jones interactions may in some cases lead to unexpected serious artifacts, and Wong-ekkabut et al.⁴⁰ found that some of the commonly used protocols may lead to deceptively beautiful but unphysical behavior, such as the spontaneous flow of water in systems containing narrow channels such as nanotubes or nanopores. Similar conclusions using different software were reached by Zuo et al.⁴¹ In addition, Ni et al.⁴² found that inappropriate treatment of electrostatic interactions produces artificial repulsions between charged residues in simulations containing DNA. This was identified as the reason behind artificial melting of double-stranded DNA. In this article, we use a membrane protein as our test system and study how the method for computing electrostatic interactions, reaction field vs particle-mesh Ewald,

choice of thermostats, and using neighbor lists and charge groups to speed up computations may change the physical behavior of the system. At the end, we will provide some recommendations for choosing a safe simulation protocol.

The most recent artifacts^{38,40,43} have been found in systems that contain narrow channels through which molecules, such as water, ions, or DNA, can move. These systems are characterized by the presence of highly anisotropic areas of higher and low density of molecules. Since such systems are of great interest in both biology and nanotechnology, it is important to assess how current methods can be used reliably in modeling them. In this study, we first tested how sensitive the simulations of a membrane protein are to parameter choices and then studied permeation of water molecules through the channel. Our results are applicable to all systems that contain narrow channels, for example, aquaporin,^{44–46} carbon nanotubes,^{4,47} and nanocontainers.⁴⁸

As our test system, we use the bacterial toxin alpha hemolysin (AHL) secreted by the human pathogen *Staphylococcus aureus*. AHL is heptameric, and its 33.2 kDa water-soluble monomers bind to susceptible cell and self-assemble to form a 232.4 kDa transmembrane pore. High-resolution X-ray crystallography⁴⁹ shows that the protein has a mushroom shape and is about 10 nm high. The main structure consists of a cap and beta-barrel stem, see Figure 1. The largest diameter inside the pore is about 4.6 nm and is located in the cap. The narrowest part is in the stem with a diameter of about 1.6 nm,⁵⁰ Figure 1. The pore is nonselective and thus allows for transport of water, ions, and small molecules.

The nonselective nature of transport exhibited by AHL is appealing for applications in biotechnology, nanotechnology,

Received: February 15, 2012

Published: June 26, 2012

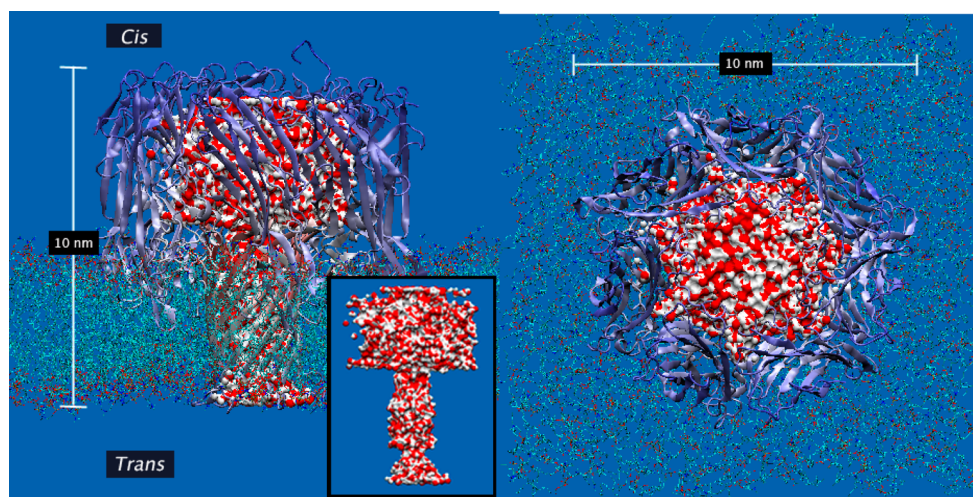


Figure 1. Snapshot from an MD simulation (a) from the side and (b) the same system as seen from above. Protein (radius gradient color ribbon) is embedded in a lipid bilayer, and water molecules (red and white) hydrate the system with a density of about 1000 kg/m^3 . Protein pore was occupied by 1426 ± 38 water molecules. (Inset) Water molecules that are inside the pore.

and medicine. Suggested applications include bombardment of cancer cells with proteins that would damage cells' outer membranes, making them susceptible to chemotherapy,⁵¹ biosensors, and DNA sequencing.^{52,53} The wild-type AHL channel shows a weak anion conductivity,^{54,55} and site-directed mutations inside the channel,^{55,56} such as K147N or M113P, can be made to tune the channel to be moderately cation selective. AHL can hence be used as a good and physically relevant test system.

MOLECULAR DYNAMICS SIMULATIONS

We performed classical MD simulations of AHL⁴⁹ embedded into a palmitoyloleoylphosphatidylcholine (POPC) lipid bilayer to study the permeation of water into the protein pore (Figure 1). The structure was taken from the protein data bank (PDB ID 7AHL).^{49,57} The Gromos 53A5 force field¹⁹ was used. We also performed simulations with Gromos53a6¹⁹ and observed no changes in the systems' behaviors.⁵⁸

AHL is protonated at neutral pH,⁵⁹ resulting in a positively (+7) charged structure. To maintain overall charge neutrality, 7 Cl^- counterions were added.⁶⁰ A pre-equilibrated lipid bilayer structure was used,⁶¹ and the double-bond parameters of POPC lipids⁶² were corrected following Bachar et al.^{11,63} The system consisted of one AHL, 401 POPC lipids, 7 Cl^- counterions, and 36 747 water molecules. For water, we used the simple point charge model (SPC).⁶⁴ The box size was $12.9 \text{ nm} \times 12.8 \text{ nm} \times 12.0 \text{ nm}$. After energy minimization using the steepest decent algorithm to remove cavities and close contacts, an equilibration MD run was performed over 100 ns. The production runs for each of the independent systems were run for 40–80 ns, and the initial structure was taken from the last state of equilibration run. This same structure (and identical setup) was used in all production simulations. Simulations were carried out with the GROMACS package version 4.0.5⁶⁵ in the NVT (constant particle number, volume, and temperature) ensemble. The integration time step was set to 1 fs, and the trajectories were saved every 2 ps for analysis. Periodic boundary conditions were applied in all directions. Protein, lipids, and water molecules were thermostatted separately at 323 K (ions were grouped with water molecules). Simulation times and details are listed in Tables 1 and 2.

Table 1. List of Simulation Parameters in the Molecular Dynamics Simulation^a

	interaction basis	temperature coupling	electrostatics calculation	frequency of neighbor list update (nlist)	time (ns)
system 1	charge group	Berendsen	reaction field	10	50
system 2	charge group	Berendsen	reaction field	1	40
system 3	charge group	Berendsen	PME	10	80
system 4	charge group	Berendsen	PME	1	80
system 5	charge group	V-rescale	PME	10	80
system 6	charge group	V-rescale	PME	1	80
system 7	atom	Berendsen	reaction field	10	50
system 8	atom	Berendsen	reaction field	1	15

^aThe frequency of neighbor list updates (nlist; specific to Gromacs). Long-range electrostatic interactions using reaction field⁶⁹ and particle-mesh Ewald (PME).^{70,71} Time refers to the length of the production simulation after 100 ns equilibration. Thermostats: Berendsen weak coupling⁷⁶ and the Parrinello–Donadio–Bussi velocity rescale.^{81,82} Charge group and atomic group^{42,65} were used as a basis to compute the interaction cut off. For charge group, default values were used.

It has been shown that simulations of nanotube systems may lead to an unphysical flow.^{40,41} To eliminate possible errors and see where they originate from, we tested different algorithms and procedures including the frequency of neighbor list updates, long-range electrostatic interactions, thermostats, and charge groups to calculate interaction cutoff. Neighbor list update and charge groups are specific to Gromacs, but the rest apply to all simulation software; the concept of charge groups in Gromacs are explained in detail in the section “Domain Decomposition” in Hess et al.,⁶⁵ and a detailed study of their effect on physical properties has been done by Wohler and Edholm.⁶⁶ The lists of simulation parameters used in MD and stochastic dynamics/Langevin dynamics (SD)⁶⁷ are shown in Tables 1 and 2, respectively. Visualizations were done using Visual Molecular Dynamics (VMD) software.⁶⁸

Table 2. List of Simulation Parameters Used in SD Simulations⁶⁷ (Langevin dynamics)^a

	temperature coupling	inverse friction constant (ps)	electrostatics calculation	frequency of neighbor list update (nlist)	time (ns)
system 9	Langevin	2	reaction field	10	50
system 10	Langevin	0.1	reaction field	10	50
system 11	Langevin	2	PME	10	50
system 12	Langevin	0.1	PME	10	50
system 13	Langevin	2	PME	1	50
system 14	Langevin	0.1	PME	1	50

^aIn all simulations, the Langevin thermostat was used to control the temperature with the inverse friction constants of 2 and 0.1 ps and default values of charge group were used. Production simulations were run for 50 ns, and the frequency of neighbor list updates (nlist) was varied between 1 and 10 steps. Long-range electrostatic interactions using reaction field⁶⁹ and particle-mesh Ewald (PME)^{70,71} were tested.

Lennard–Jones interactions with a cutoff radius of 1.0 nm were applied in all simulations. For electrostatics interactions, we compared the reaction field⁶⁹ and particle-mesh Ewald (PME) methods.^{70,71} In simulations using the reaction field method, all electrostatic interactions were explicitly computed within a cutoff radius of 2.0 nm. Beyond the cutoff a dielectric constant of 62 was used.⁷² The cutoff used here is very conservative as very commonly either 1.2 and 1.8 nm is used. Simulations with shorter cutoffs than the one used here accentuate the observed artifacts. These issues are general to all simulation software using reaction field electrostatics.

In the simulations using the PME method, a direct space cutoff of 1.0 nm was applied. In the calculation of long-range contribution in reciprocal space, we used cubic interpolation of order four using a maximum spacing of 1.2 Å for the FFT grid and the relative strength of the electrostatic interaction at the cutoff was 10^{-5} .

SIMULATION RESULTS AND DISCUSSIONS

1. Unphysical Unidirectional Flow. We first examine the possible appearance of unphysical flow and its dependence on simulation parameters as seen in an analogous carbon nanotube system.⁴⁰ Issues concerning the different thermostats and methods for computing the electrostatic interactions are common to all simulation software, such as Gromacs,⁶⁵ CHARMM,⁷³ Amber,⁷⁴ Espresso,⁷⁵ and so on. As mentioned above, charge groups and tunable neighbor list update frequency are specific to Gromacs.⁶⁵ In brief, a charge group is a small set of nearby atoms that are grouped together. Computation of electrostatic interactions is based on the distance from the geometric center of this group: If a neighbor that does not belong to a group is farther away from the geometric center of the charge group than the cutoff distance, its direct electrostatic interactions are not computed with any of the atoms belonging to the group even if the distance to some of the members of the group is shorter than the cutoff length. This can provide a significant speed up and is conceptually simple, but charge groups have to be used very carefully in order to avoid physical artifacts.⁴⁰ As a default, Gromacs neighbor lists are updated every 10 time steps (parameter nlist

= 10). Although this is often a safe choice, it may lead to unphysical behavior in highly anisotropic systems since interactions could be missing from the calculation when lists were not sufficiently updated. The problem is that wrong choices do not lead to an unstable simulation: The algorithm remains stable, but the results are physically wrong. The only way to ensure the correctness of parameters is to perform tests of significant length. In our experience, the minimum length of such tests is at least tens of nanoseconds.

Case 1: Effect of Neighbor Lists and Reaction Field Electrostatics.⁶⁹ We will examine each system in detail. The labels “system 1” and so on refer to the systems in Table 1.

- System 1: Neighbor list update was set to 10 (default value in Gromacs). The Berendsen weak coupling thermostat⁷⁶ and reaction field electrostatics⁶⁹ were applied. Default charge groups were used. We tracked the number of water molecules flowing from cis to trans and vice versa. Figure 2 shows that this combination

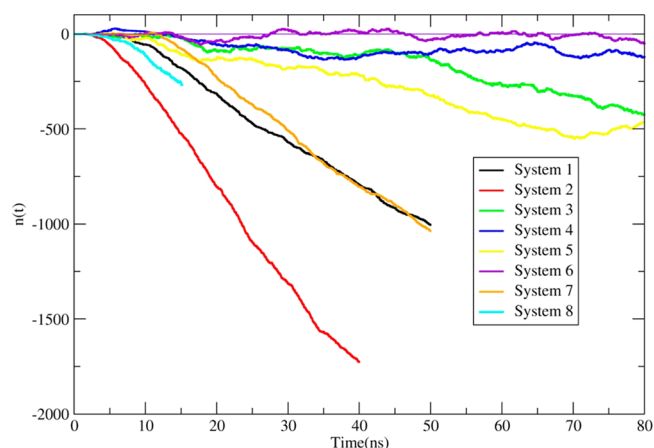


Figure 2. Net number of water molecules (n) successfully permeated from cis to trans as a function of time in MD simulations. Simulation parameters for each system are provided in Table 1.

leads to an artificial flow. In our production simulation, 942 water molecules were transported from the cis to the trans side and only 148 moved in the opposite direction.

- System 2: As in system 1, but instead of setting nlist = 10, we updated the neighbor lists at every time step (nlist = 1). This is the typical setup in software other than Gromacs. Somewhat surprisingly, the net flux was found to be even larger than for nlist = 10. We could not clearly identify the reason for the increase of the net flux, but the main reason for it is in reaction field electrostatics.

Case 2: Reaction Field vs Particle-Mesh Ewald. The next possible error source is calculation of the long-range electrostatic interactions. There are three main approaches to treating electrostatic interactions: truncated electrostatics, Ewald summation-based methods, and reaction field which is essentially truncation plus mean field correction. A review of different methods is provided by Karttunen et al.²⁴ First, possible artificial periodicity is largely attenuated in the reaction field approach, but this has been debated in the past several years.⁷⁷ Second, the reaction field method for electrostatics offers a reduction in the computer time required by assuming a uniform dielectric constant of water beyond the short-range cutoff value. As parallelization of the FFT has become more efficient, PME has become very competitive against the

reaction field⁷⁸ if a long cutoff is used in reaction field, PME become computationally faster.⁷⁸ The reaction field approach requires the dielectric constant as an input. In real systems the dielectric constant is, however, not homogeneous and may lead to errors. At the cutoff there is also a discontinuity in the electrostatic potential, and this may create an artificial force.^{79,80} Therefore, the particle-mesh Ewald (PME) technique^{70,71} should be used instead of the reaction field method.^{24,27,78}

- System 3: The simulation was run with the same parameters as in system 1 ($nlist = 10$), except that PME was used instead of the reaction field method. The results show that the net flux is significantly reduced compared to the reaction field simulations. The net flux in the production simulation was 423 water molecules transported from the cis to the trans side.
- System 4: $nlist = 1$. As with system 2, this setup is typical in software other than Gromacs. The net flux nearly disappeared (Figure 2): PME electrostatics is clearly preferable to reaction field.

Case 3: Effect of Thermostat. In this case, we used the same setups as in systems 3 and 4 but instead of the Berendsen weak coupling thermostat⁷⁶ we used the Parrinello–Donadio–Bussi velocity rescale thermostat.^{81,82}

- System 5: $nlist = 10$, PME electrostatics. The behavior was very similar to system 3.
- System 6: $nlist = 1$, PME electrostatics. The net flux disappeared. Comparison with system 4 shows that the thermostat clearly has an effect and that the velocity rescale thermostat is the preferred choice. Comparison of systems 5 and 3 shows that errors due to the neighbor list updates and thermostat are not easily separable into distinct contributions.

Case 4: Charge Groups vs No Charge Groups. We compared the effect of removing charge groups using the worst cases from the above in order to gain more insight into the different error sources. We used the systems from case 1, i.e., reaction field electrostatics and the Berendsen weak coupling thermostat. In terms of computational efficiency, simulations using atom-based truncation with $nlist = 1$ are remarkably expensive, approximately an order of magnitude slower than using $nlist = 10$ (with atom based, i.e., no charge groups).

- System 7: $nlist = 10$, no charge groups. The observed behavior was very similar to system 1; the net flux converged approximately to the same value, although the flux started later.
- System 8: $nlist = 1$, no charge groups. We did not run this simulation further than about 15 ns, but there is a clear improvement compared to system 2 (the same system with default charge groups).

Case 5: Simulations Using Stochastic Dynamics. Finally, we performed SD simulations (Figure 3) in order to ensure that the velocities of particles in the system were generated in the correct ensemble.

- Systems 9 and 10: Parameters similar to system 1 were used (reaction field electrostatics, $nlist = 10$). Inverse friction coefficients of 2 and 0.1 ps were applied to the systems 9 and 10, respectively. The observed behavior was very similar to the MD simulations of systems 1 and 2, i.e., a net flux appeared. The flux was smaller with smaller inverse friction coefficient; the dynamics of the

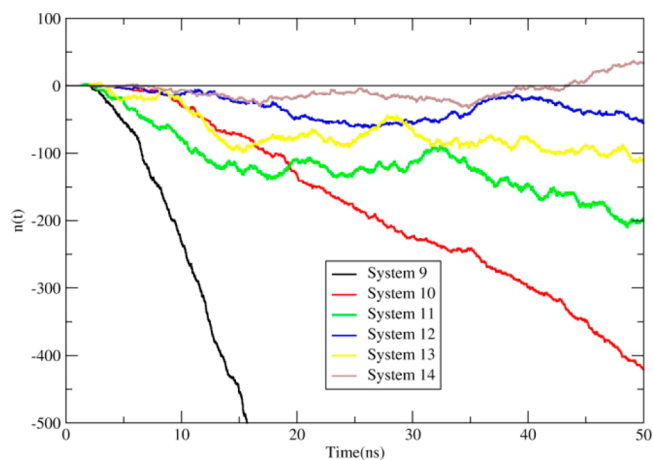


Figure 3. Net number of water molecules (n) successfully permeated from cis to trans as a function of time in SD simulations. Simulation parameters for each system can be seen in Table 2.

water molecules is damped by a high friction coefficient (smaller inverse friction).

- Systems 11 and 12: PME electrostatics was used instead of reaction field. The neighbor lists were updated every 10 time steps, and again, inverse friction coefficients of 2 and 0.1 ps were used in systems 11 and 12, respectively. Similar to the previous MD simulations, the net flux was significantly reduced in comparison to systems 9 and 10, and it almost disappeared when an inverse friction coefficient of 0.1 was used.
- Systems 13 and 14: The neighbor lists were updated every time step. Inverse friction coefficients of 2 and 0.1 ps were used in systems 13 and 14, respectively. The net flux disappeared in system 14. This is consistent with the results from system 6, MD with the velocity rescale thermostat. This is also similar to the results reported by Zuo et al.⁴¹ using NAMD software.⁸³

2. Pore Shape and Water in Confined Geometry. As a brief application we studied the density of water inside the pore. On the basis of the previous section, we chose charge group-based electrostatic interactions, V-rescale thermostat, PME, and $nlist = 1$ (system 6) to ensure that the simulation setup is physically correct. We used charge groups instead of atoms based for speed since system 6 showed no artifacts. We started by analyzing the water density within the pore. The results are based on an 80 ns production simulation and shown in Figure 4. The error bars are given by the standard deviation. The profile in Figure 4A is consistent with previous work.^{54,84} It is also comparable with the open state of the mechanosensitive channel of a large conductance protein (MSL) channel.⁸⁵ The AHL protein pore has a funnel-like shape with a wide cap ($6.3 < z < 10.5$ nm) and a narrow stem ($1.5 < z < 6.3$ nm). The narrowest and widest radii inside the pore were measured to be 0.79 ± 0.08 and 2.07 ± 0.09 nm at $z = 6.3$ and 7.5 nm from the simulation box bottom (or a distance of 4.8 and 6.0 nm from the end of the protein stem), respectively. The protein pore was occupied by a total of 1426 ± 38 water molecules. Water density in the cap region is close to the bulk density of water, but in the stem the density is significantly lower. Moreover, in the stem region there are two density minima: 548 ± 93 kg/m³ at $z = 2.7$ nm and 526 ± 86 kg/m³ at $z = 5.7$ nm. These are the locations of the hydrophobic residues, leucine (Leu135, Leu428, Leu721, Leu1014, Leu1307, Leu1600, and Leu1893)

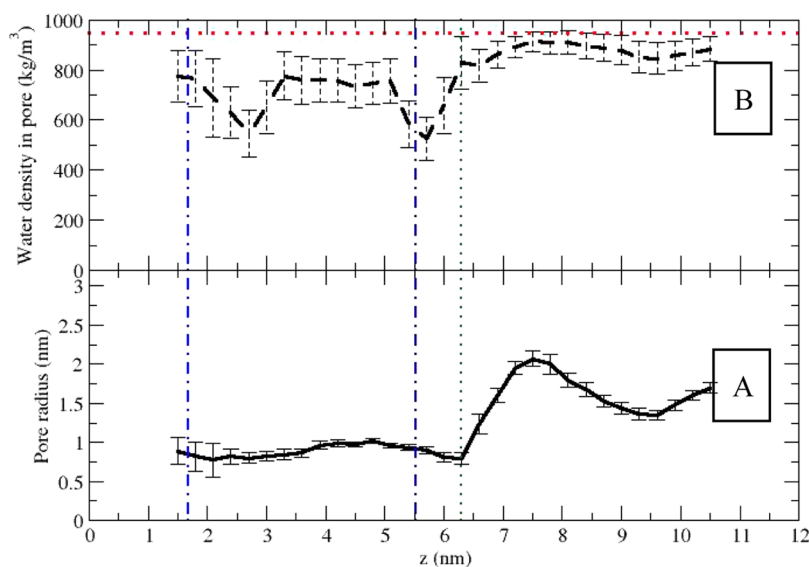


Figure 4. Pore radius (A) and water density inside the channel (B). Red dotted line: bulk water density. Blue dot–dashed lines represent the average phosphate locations of the lipids in the lipid bilayer. Constriction (the narrowest pore radius) is indicated by the green dotted line.

and methionine (Met113, Met406, Met699, Met992, Met1285, Met1578, and Met1871), respectively. These two minima were also observed by Cozmuta et al.⁸⁴ A decrease in water density has also been shown in neutral and irregularly charged carbon nanotubes.^{86–88} According to MD simulations,^{87,88} the carbon nanotube channel was filled with a tubular-like water structure at a central water core having near-randomly distributed molecules due to thermal movement. It has also been found that water density decreases as the pore diameter decreases. The water density in the stem is equal to the density of water in a 2 nm diameter carbon nanotube.⁸⁷ We did not, however, observe the reported tubular-like^{87,88} water structure inside this protein channel.

CONCLUSIONS

We performed atomistic MD and SD simulations to investigate error sources and define a safe protocol for simulations of systems containing pores and channels. We used an AHL protein embedded into a lipid bilayer as model and investigated the permeation of water molecules through the protein channel. We found that an artificial unidirectional flow was mainly related to neighbor list update, calculation of electrostatic interactions, and choice of thermostat. The unidirectional flow was significantly reduced when PME was used, and neighbor lists were updated at every time step. When the Parrinello–Donadio–Bussi V-rescale^{81,82} thermostat was used (with the above protocol) instead of the Berendsen weak coupling thermostat⁷⁶ the unidirectional flow disappeared. On the basis of our findings, we recommend the following.

- Tests should be run over a sufficiently long time. Some of the errors manifest themselves only after tens of nanoseconds: The results in Figure 1 were preceded by 100 ns of equilibration, and even then there was an offset time.
- PME electrostatics should always be preferred over reaction field, and cutoff should be avoided altogether. Even with a long cutoff, such as that tested here, reaction field electrostatics leads to unpredictable behavior; mean field is not a good description for systems containing pore-like structures.

- Stochastic or local thermostats should be used. Global thermostats, these apply the same change everywhere at the same moment, are fine in bilayer systems, but in systems containing areas with small numbers of water, such as in pores, they seem to introduce deviations and lead to creation of artificial temperature gradients. The Parrinello–Donadio–Bussi V-rescale thermostat^{81,82} combines a stochastic component with a global (Berendsen weak coupling⁷⁶) thermostat. Both here and in other studies⁴⁰ it has shown excellent behavior. It is already implemented in Gromacs.⁶⁵ NAMD⁸³ includes the Lowe–Andersen thermostat⁸⁹ that is local and momentum conserving and has been shown to perform well in dissipative particle dynamics simulations.^{89,90}
- If an option for neighbor list updates exists, it should be set to 1 (nlist = 1). In Gromacs the default is nlist = 10, that is, in our experience, safe in lipid bilayer simulations but not for systems containing pores.
- Charge groups: This is specific to the GROMOS force field and Gromacs; to our knowledge, GROMOS simulation software⁹¹ also uses them (we did not have access to GROMOS software and could not test it). NAMD⁸³ and LAMPPS⁹² are able to use the GROMOS force field, but they do not utilize charge groups. We observed that if neighbor lists are updated at each time step, the default charge groups in GROMOS 53A5¹⁹ do not introduce artifacts. With nlist = 10, however, significant unphysical artifacts were observed. When creating topologies for different systems, great care should be applied in keeping charge groups small as too large charge groups can lead to very significant errors as reported by Wong-ekkabut et al.⁴⁰

Finally, we would like to point out that the software and force fields used here, as well as the other ones mentioned here, have been tested in other studies, and they have been shown to be capable of producing reliable results.^{19,58,93,94} Force-field development and reliability are among the core issues in achieving more reliable simulations.^{21,95} It is, however, always the user's responsibility to check the correctness of the protocols and methods even if it is time consuming.

■ AUTHOR INFORMATION

Corresponding Author

*E-mail: jirasak.w@ku.ac.th; mikko.karttunen@uwaterloo.ca.

Notes

The authors declare no competing financial interest.

■ ACKNOWLEDGMENTS

We would like to thank Dr. Markus Miettinen for helpful discussions. Financial support was provided by the Thailand Research Fund (TRF; J.W.), Kasetsart University Research and Development Institute (KURDI; J.W.), the Faculty of Science at Kasetsart University (J.W.), the Natural Sciences and Engineering Research Council of Canada (M.K.), and the Ontario Early Researcher Award program (M.K.). Computational resources were provided by SHARCNET (www.sharcnet.ca) and the Department of Physics, Faculty of Science, Kasetsart University.

■ REFERENCES

- (1) Klepeis, J. L.; Lindorff-Larsen, K.; Dror, R. O.; Shaw, D. E. *Curr. Opin. Struct. Biol.* **2009**, *19*, 120–127.
- (2) Schlick, T.; Collepardo-Guevara, R.; Halvorsen, L. A.; Jung, S.; Xiao, X. Q. *Rev. Biophys.* **2011**, *44*, 191–228.
- (3) Lyubartsev, A. P.; Rabinovich, A. L. *Soft Matter* **2011**, *7*, 25–39.
- (4) Hummer, G.; Rasaiah, J. C.; Noworyta, J. P. *Nature* **2001**, *414*, 188–190.
- (5) Busch, S.; Smuda, C.; Pardo, L. C.; Unruh, T. *J. Am. Chem. Soc.* **2010**, *132*, 3232–3233.
- (6) Falck, E.; Rog, T.; Karttunen, M.; Vattulainen, I. *J. Am. Chem. Soc.* **2008**, *130*, 44–45.
- (7) Holt, J. K.; Park, H. G.; Wang, Y. M.; Stadermann, M.; Artyukhin, A. B.; Grigoropoulos, C. P.; Noy, A.; Bakajin, O. *Science* **2006**, *312*, 1034–1037.
- (8) Stimson, L.; Dong, L.; Karttunen, M.; Wisniewska, A.; Dutka, M.; Rog, T. *J. Phys. Chem. B* **2007**, *111*, 12447–12453.
- (9) Repakova, J.; Holopainen, J. M.; Karttunen, M.; Vattulainen, I. *J. Phys. Chem. B* **2006**, *110*, 15403–15410.
- (10) Lippert, R. A.; Bowers, K. J.; Dror, R. O.; Eastwood, M. P.; Gregersen, B. A.; Klepeis, J. L.; Kolossvary, I.; Shaw, D. E. *J. Chem. Phys.* **2007**, *126*, 046101.
- (11) Martinez-Seara, H.; Rog, T.; Karttunen, M.; Reigada, R.; Vattulainen, I. *J. Chem. Phys.* **2008**, *129*, 105103.
- (12) Ono, S.; Kuroda, M.; Higo, J.; Kamiya, N.; Nakajima, N.; Nakamura, H. *J. Biol. Phys.* **2002**, *28*, 427–437.
- (13) Hegefeld, W. A.; Chen, S. E.; DeLeon, K. Y.; Kuczera, K.; Jas, G. S. *J. Phys. Chem. A* **2010**, *114*, 12391–12402.
- (14) Soares, T. A.; Daura, X.; Oostenbrink, C.; Smith, L. J.; van Gunsteren, W. F. *J. Biomol. NMR* **2004**, *30*, 407–422.
- (15) Schmid, N.; Eichenberger, A. P.; Choutko, A.; Riniker, S.; Winger, M.; Mark, A. E.; van Gunsteren, W. F. *Eur. Biophys. J.* **2011**, *40*, 843–856.
- (16) Auffinger, P.; Cheatham, T. E.; Vaiana, A. C. *J. Chem. Theory Comput.* **2007**, *3*, 1851–1859.
- (17) Best, R. B.; Buchete, N. V.; Hummer, G. *Biophys. J.* **2008**, *95*, 7–9.
- (18) Cao, Z.; Liu, L.; Wang, J. *J. Biomol. Struct. Dyn.* **2011**, *29*, 527–539.
- (19) Oostenbrink, C.; Villa, A.; Mark, A. E.; Van Gunsteren, W. F. *J. Comput. Chem.* **2004**, *25*, 1656–1676.
- (20) Ulmschneider, J. P.; Ulmschneider, M. B. *J. Chem. Theory Comput.* **2009**, *5*, 1803–1813.
- (21) Piana, S.; Lindorff-Larsen, K.; Shaw, D. E. *Biophys. J.* **2011**, *100*, 47–49.
- (22) Anezo, C.; de Vries, A. H.; Holtje, H. D.; Tieleman, D. P.; Marrink, S. J. *J. Phys. Chem. B* **2003**, *107*, 9424–9433.
- (23) Norberg, J.; Nilsson, L. *Biophys. J.* **2000**, *79*, 1537–1553.
- (24) Karttunen, M.; Rottler, J.; Vattulainen, I.; Sagui, C. *Curr. Top. Membr.* **2008**, *60*, 49–89.
- (25) Fennell, C. J.; Gezelter, J. D. *J. Chem. Phys.* **2006**, *124*, 234104.
- (26) Feller, S. E.; Pastor, R. W.; Rojnuckarin, A.; Bogusz, S.; Brooks, B. R. *J. Phys. Chem.* **1996**, *100*, 17011–17020.
- (27) Patra, M.; Karttunen, M.; Hyvonen, M. T.; Falck, E.; Vattulainen, I. *J. Phys. Chem. B* **2004**, *108*, 4485–4494.
- (28) Hardy, D. J.; Stone, J. E.; Schulten, K. *Parallel Comput.* **2009**, *35*, 164–177.
- (29) Yonetani, Y. *Chem. Phys. Lett.* **2005**, *406*, 49–53.
- (30) Patra, M.; Karttunen, M.; Hyvonen, M. T.; Falck, E.; Lindqvist, P.; Vattulainen, I. *Biophys. J.* **2003**, *84*, 3636–3645.
- (31) Tobias, D. J. *Curr. Opin. Struct. Biol.* **2001**, *11*, 253–261.
- (32) Sagui, C.; Pedersen, L. G.; Darden, T. A. *J. Chem. Phys.* **2004**, *120*, 73–87.
- (33) Ballenegger, V.; Arnold, A.; Cerda, J. J. *J. Chem. Phys.* **2009**, *131*, 094107.
- (34) Mark, P.; Nilsson, L. *J. Comput. Chem.* **2002**, *23*, 1211–1219.
- (35) Gurtovenko, A. A.; Vattulainen, I. *J. Chem. Phys.* **2009**, *130*, 215107.
- (36) Gargallo, R.; Oliva, B.; Querol, E.; Aviles, F. X. *Protein Eng.* **2000**, *13*, 21–26.
- (37) Gargallo, R.; Hunenberger, P. H.; Aviles, F. X.; Oliva, B. *Protein Sci.* **2003**, *12*, 2161–2172.
- (38) Bonthuis, D. J.; Rinne, K. F.; Falk, K.; Nadir Kaplan, C.; Horinek, D.; Nihat Berker, A.; Bocquet, L.; Netz, R. R. *J. Phys.: Condens. Matter* **2011**, *23*, 184110.
- (39) Bonthuis, D. J.; Horinek, D.; Bocquet, L.; Netz, R. R. *Phys. Rev. Lett.* **2009**, *103*, 144503.
- (40) Wong-Ekkabut, J.; Miettinen, M. S.; Dias, C.; Karttunen, M. *Nat. Nanotechnol.* **2010**, *5*, 555–557.
- (41) Zuo, G.; Shen, R.; Ma, S.; Guo, W. *ACS Nano* **2010**, *4*, 205–210.
- (42) Ni, B.; Baumketner, A. *J. Mol. Model.* **2011**, 1–11.
- (43) Bonthuis, D. J.; Falk, K.; Kaplan, C. N.; Horinek, D.; Berker, A. N.; Bocquet, L.; Netz, R. R. *Phys. Rev. Lett.* **2010**, *105*, 209401.
- (44) de Groot, B. L.; Grubmuller, H. *Science* **2001**, *294*, 2353–2357.
- (45) Tajkhorshid, E.; Nollert, P.; Jensen, M. O.; Miercke, L. J.; O’Connell, J.; Stroud, R. M.; Schulten, K. *Science* **2002**, *296*, 525–530.
- (46) Zhu, F. Q.; Tajkhorshid, E.; Schulten, K. *Biophys. J.* **2004**, *86*, 50–57.
- (47) Beckstein, O.; Sansom, M. S. P. *Proc. Natl. Acad. Sci. U.S.A.* **2003**, *100*, 7063–7068.
- (48) Cisse, I.; Okumus, B.; Joo, C.; Ha, T. *J. Proc. Natl. Acad. Sci. U.S.A.* **2007**, *104*, 12646–12650.
- (49) Song, L. Z.; Hobaugh, M. R.; Shustak, C.; Cheley, S.; Bayley, H.; Gouaux, J. E. *Science* **1996**, *274*, 1859–1866.
- (50) Gouaux, E. *J. Struct. Biol.* **1998**, *121*, 110–122.
- (51) Panchal, R. G.; Cusack, E.; Cheley, S.; Bayley, H. *Nat. Biotechnol.* **1996**, *14*, 852–856.
- (52) Dekker, C. *Nat. Nanotechnol.* **2007**, *2*, 209–215.
- (53) Kasianowicz, J. J.; Brandin, E.; Branton, D.; Deamer, D. W. *Proc. Natl. Acad. Sci. U.S.A.* **1996**, *93*, 13770–13773.
- (54) Aksimentiev, A.; Schulten, K. *Biophys. J.* **2005**, *88*, 3745–3761.
- (55) Noskov, S. Y.; Im, W.; Roux, B. *Biophys. J.* **2004**, *87*, 2299–2309.
- (56) Gu, L. Q.; Cheley, S.; Bayley, H. *J. Gen. Physiol.* **2001**, *118*, 481–493.
- (57) Bernstein, F. C.; Koetzle, T. F.; Williams, G. J. B.; Meyer, E. F.; Brice, M. D.; Rodgers, J. R.; Kennard, O.; Shimanouchi, T.; Tasumi, M. *J. Mol. Biol.* **1977**, *112*, 535–542.
- (58) Olubiyi, O. O.; Strodel, B. *J. Phys. Chem. B* **2012**, *116*, 3280–3291.
- (59) Kasianowicz, J. J.; Misakian, M. *J. Membr. Biol.* **2003**, *195*, 137–146.
- (60) Patra, M.; Karttunen, M. *J. Comput. Chem.* **2004**, *25*, 678–689.
- (61) Tieleman, D. P.; Berendsen, H. J. C. *J. Chem. Phys.* **1996**, *105*, 4871–4880.

- (62) Berger, O.; Edholm, O.; Jahnig, F. *Biophys. J.* **1997**, *72*, 2002–2013.
- (63) Bachar, M.; Brunelle, P.; Tieleman, D. P.; Rauk, A. *J. Phys. Chem. B* **2004**, *108*, 7170–7179.
- (64) Berendsen, H. J. C.; Postma, J. P. M.; van Gunsteren, W. F.; Hermans, J. In *Intermolecular Forces*; Pullman, B., Ed.; D. Reidel: Dordrecht, The Netherlands, 1981; pp 331–342.
- (65) Hess, B.; Kutzner, C.; van der Spoel, D.; Lindahl, E. *J. Chem. Theory Comput.* **2008**, *4*, 435–447.
- (66) Wohllert, J.; Edholm, O. *Biophys. J.* **2004**, *87*, 2433–2445.
- (67) van Gunsteren, W. F.; Berendsen, H. J. C. *Mol. Simul.* **1988**, *1*, 173–185.
- (68) Humphrey, W.; Dalke, A.; Schulten, K. *J. Mol. Graphics* **1996**, *14*, 33–38.
- (69) Tironi, I. G.; Sperb, R.; Smith, P. E.; Vangunsteren, W. F. *J. Chem. Phys.* **1995**, *102*, 5451–5459.
- (70) Essmann, U.; Perera, L.; Berkowitz, M. L.; Darden, T.; Lee, H.; Pedersen, L. G. *J. Chem. Phys.* **1995**, *103*, 8577–8593.
- (71) Darden, T.; York, D.; Pedersen, L. *J. Chem. Phys.* **1993**, *98*, 10089–10092.
- (72) Ng, J. A.; Vora, T.; Krishnamurthy, V.; Chung, S. H. *Eur. Biophys. J.* **2008**, *37*, 213–222.
- (73) Brooks, B. R.; Brooks, C. L.; Mackerell, A. D.; Nilsson, L.; Petrella, R. J.; Roux, B.; Won, Y.; Archontis, G.; Bartels, C.; Boresch, S.; Cafilisch, A.; Caves, L.; Cui, Q.; Dinner, A. R.; Feig, M.; Fischer, S.; Gao, J.; Hodoscek, M.; Im, W.; Kuczera, K.; Lazaridis, T.; Ma, J.; Ovchinnikov, V.; Paci, E.; Pastor, R. W.; Post, C. B.; Pu, J. Z.; Schaefer, M.; Tidor, B.; Venable, R. M.; Woodcock, H. L.; Wu, X.; Yang, W.; York, D. M.; Karplus, M. *J. Comput. Chem.* **2009**, *30*, 1545–1614.
- (74) Case, D. A.; Cheatham, T. E.; Darden, T.; Gohlke, H.; Luo, R.; Merz, K. M.; Onufriev, A.; Simmerling, C.; Wang, B.; Woods, R. J. *J. Comput. Chem.* **2005**, *26*, 1668–1688.
- (75) Limbach, H. J.; Arnold, A.; Mann, B. A.; Holm, C. *Comput. Phys. Commun.* **2006**, *174*, 704–727.
- (76) Berendsen, H. J. C.; Postma, J. P. M.; Vangunsteren, W. F.; Dinola, A.; Haak, J. R. *J. Chem. Phys.* **1984**, *81*, 3684–3690.
- (77) Kastenzholz, M. A.; Hunenberger, P. H. *J. Phys. Chem. B* **2004**, *108*, 774–788.
- (78) Patra, M.; Hyvonen, M. T.; Falck, E.; Sabouri-Ghomi, M.; Vattulainen, I.; Karttunen, M. *Comput. Phys. Commun.* **2007**, *176*, 14–22.
- (79) Toxvaerd, S.; Dyre, J. C. *J. Chem. Phys.* **2011**, *134*, 081102.
- (80) Baumketner, A. *J. Chem. Phys.* **2009**, *130*, 104106.
- (81) Bussi, G.; Donadio, D.; Parrinello, M. *J. Chem. Phys.* **2007**, *126*, 014101.
- (82) Bussi, G.; Zykova-Timan, T.; Parrinello, M. *J. Chem. Phys.* **2009**, *130*, 074101.
- (83) Phillips, J. C.; Braun, R.; Wang, W.; Gumbart, J.; Tajkhorshid, E.; Villa, E.; Chipot, C.; Skeel, R. D.; Kale, L.; Schulten, K. *J. Comput. Chem.* **2005**, *26*, 1781–1802.
- (84) Cozmuta, I.; O’Keeffe, J. T.; Bose, D.; Stolc, V. *Mol. Simul.* **2005**, *31*, 79–93.
- (85) Tang, Y.; Yoo, J.; Yethiraj, A.; Cui, Q.; Chen, X. *Biophys. J.* **2008**, *95*, 581–596.
- (86) Banerjee, S.; Murad, S.; Puri, I. K. *Chem. Phys. Lett.* **2007**, *434*, 292–296.
- (87) Hennrich, F.; Arnold, K.; Lebedkin, S.; Quintilla, A.; Wenzel, W.; Kappes, M. M. *Phys. Status Solidi B* **2007**, *244*, 3896–3900.
- (88) Huang, B.; Xia, Y.; Zhao, M.; Li, F.; Liu, X.; Ji, Y.; Song, C. *J. Chem. Phys.* **2005**, *122*, 84708.
- (89) Koopman, E. A.; Lowe, C. P. *J. Chem. Phys.* **2006**, *124*, 204103.
- (90) Nikunen, P.; Karttunen, M.; Vattulainen, I. *Comput. Phys. Commun.* **2003**, *153*, 407–423.
- (91) Christen, M.; Hunenberger, P. H.; Bakowies, D.; Baron, R.; Burgi, R.; Geerke, D. P.; Heinz, T. N.; Kastenzholz, M. A.; Krautler, V.; Oostenbrink, C.; Peter, C.; Trzesniak, D.; van Gunsteren, W. F. *J. Comput. Chem.* **2005**, *26*, 1719–1751.
- (92) Plimpton, S. J. *Comput. Phys.* **1995**, *117*, 1–19.
- (93) Oostenbrink, C.; Soares, T. A.; van der Vegt, N. F.; van Gunsteren, W. F. *Eur. Biophys. J.* **2005**, *34*, 273–284.
- (94) Cino, E. A.; Wong-ekkabut, J.; Karttunen, M.; Choy, W. Y. *PLoS One* **2011**, *6*, 27371.
- (95) Beauchamp, K. A.; Lin, Y. S.; Das, R.; Pande, V. S. *J. Chem. Theory Comput.* **2012**, *8*, 1409–1414.